Frangulea, George V., Assimakopoulos, Philippos, Bojović, Biljana and Lagén, Sandra (2025) *NR-U and Wi-Fi Unlicensed Spectrum Sharing: Design Challenges and Solutions*. Computer Communications, 237 . ISSN 0140-3664.

Computer Communications 237 (2025) 108143

Contents lists available at ScienceDirect

Computer Communications

journal homepage: www.elsevier.com/locate/comcom

NR-U and Wi-Fi Unlicensed Spectrum Sharing: Design Challenges and Solutions

George V. Frangulea [a],*, Philippos Assimakopoulos [a], Biljana Bojović [b], Sandra Lagén [b]

[a] School of Engineering, University of Kent, Canterbury, Kent, United Kingdom
[b] Open Simulations Department, Centre Tecnològic de Telecomunicacions de Catalunya (CTTC/CERCA), Castelldefels, Barcelona, Spain

ARTICLE INFO

Keywords:
NR-U
IEEE 802.11
LBT
eXtended Reality
Spectrum sharing
Wireless coexistence

ABSTRACT

This paper presents an in-depth analysis of the Listen-Before-Talk (LBT) procedures required for cellular technologies operating in the unlicensed spectrum. We specifically investigate the 5G New Radio Unlicensed Standalone (NR-U SA) design under the most recent 3GPP standard-compliant Type 1 Channel Access Procedure (CAP). We highlight and address key challenges in adapting the asynchronous Type 1 CAP (i.e., load-based CAP) to NR-U's synchronous slot-based framework and propose the Scheduled Type 1 CAP, which introduces a novel scheduling mechanism and implementation of additional sensing to facilitate seamless integration. We carry out our performance evaluation using a full-stack end-to-end network simulator and construct a realistic 3GPP-compliant coexistence scenario in which 5G NR-U SA and Wi-Fi networks operate indoors in unlicensed sub-7 GHz bands. The users of the 5G NR-U SA and Wi-Fi networks demand eXtended Reality applications. Through an extensive evaluation study, we analyse the interplay between the NR-U numerologies and the CAPs used in shared channel access and evaluate their impact on the end-to-end performance of both technologies by considering various quality of service metrics. The results reveal some of the main pitfalls of the LBT procedure defined by 3GPP in TS 37.213 and demonstrate the clear advantages of the proposed Scheduled Type 1 CAP. Our work provides valuable insights into CAPs for shared spectrum, proposes standard-compliant solutions, and lays the groundwork for future research by introducing a pioneering open-source network simulation platform for evaluating NR-U SA coexistence scenarios with the Scheduled Type 1 CAP.

1. Introduction

As the demand for network connectivity continues its exponential growth, the advancement of fifth-generation (5G) systems faces the critical task of surpassing the performance standards set by preceding generations. Key objectives include not only higher capacity and data rates but also the imperative of low latency, presenting a multifaceted challenge in meeting the evolving needs of modern communication systems. Acknowledging this need, the Third Generation Partnership Project (3GPP) initially leveraged the Unlicensed National Information Infrastructure (UNII) bands, specifically targeting bands at 5 GHz, 6 GHz, and the millimetre Wave (mmWave) bands at 60 GHz and above [1]. While lower bands may lack sufficient capacity, and higher mmWave bands face economic and practical barriers, the 6 GHz spectrum offers a balance by providing both coverage expansion and ample capacity, making it crucial for realising the full potential of 5G networks [2]. Wireless systems can operate across shared bands, provided they adhere to spectrum-sharing regulations designed to ensure the coexistence of different wireless technologies within these bands.

During the development of 5G's predecessors, various solutions were explored, including Long-Term Evolution (LTE) Unlicensed (LTE-U) and LTE Licensed-Assisted Access (LTE-LAA) [3]. Initially, the Carrier Sensing Adaptive Transmission (CSAT) [4] cycling-based scheme was adopted for LTE-U to ensure fair coexistence with Wi-Fi networks. However, this approach was limited to areas where Listen-Before-Talk (LBT) was not mandatory for operation in the shared spectrum. In pursuit of a more versatile solution, 3GPP initially proposed two versions of asynchronous (i.e., load-based) LBT-based channel access, resembling the Carrier-Sense Multiple Access with Collision Avoidance (CSMA/CA)-based Distributed Coordination Function (DCF) in IEEE 802.11 [5]. The first version, known as Category 4 and referred to as Cat4 (Rel13) in this study, was introduced in 3GPP Technical Report (TR) 36.889 [3] in 2015 and was based on ETSI's Harmonized European Standard (EN 301.893) V1.8.1 [6]. However, in 2017, when ETSI updated regulations in V.2.1.1 [7], Cat4 ceased being compliant. To ensure LTE-LAA compliance for deployment in the shared spectrum, in 2017, 3GPP adopted the LBT mechanism detailed in EN 301 983

* Corresponding author.
E-mail address: gvf3@kent.ac.uk (G.V. Frangulea).

https://doi.org/10.1016/j.comcom.2025.108143
Received 17 October 2024; Received in revised form 21 January 2025; Accepted 8 March 2025
Available online 17 March 2025

V2.1.1. by defining Type 1 Channel Access Procedure (CAP) in Technical Specification (TS) 36.213 [8]. Despite the new regulation on LBT, much of the research on this topic continues to rely on the non-compliant version of LBT, as also highlighted in [9]. Therefore, we included Cat4 in our analysis to demonstrate the degradation it causes to the coexisting network. During the standardisation of New Radio Unlicensed (NR-U) [10], the LTE-LAA LBT procedure was deemed a baseline for the 5 GHz bands and a starting point for designing the LBT procedure for the 6 GHz band. In 2018, 3GPP initiated TS 37.213 [11], encompassing both NR-U and LTE-LAA CAPs in compliance with EN 301 893 V2.1.1. Throughout this study, the term *shared spectrum* reflects 3GPP's latest terminology to accommodate varying regulatory classifications.

The NR-U technology has gained renewed attention with the expansion of its applications to Sidelink Unlicensed (SL-U) channels in TS 37.213 Release 18 [11], as well as increased recognition for future wireless systems [12–14]. Real-world deployments are beginning to emerge, underscoring its growing importance. For instance, AI-LINK [15] and State Grid Corporation of China (SGCC) [16] have developed private 5G NR-U, operating over the n46 (5.8 GHz) unlicensed band to support video surveillance, mobile inspection robots, and other 5G-connected applications.

Despite numerous studies on NR-U/Wi-Fi channel access procedure and coexistence, key research gaps remain. Many current studies rely on outdated, non-compliant Cat4 LBT, Pei et al. [17,18,19], Zhou et al. [20], Wang et al. [21], Xiao et al. [22] and Parvini et al. [23]. Additionally, studies such as Hirzallah et al. [24] and Muhammad et al. [9] focus on NR-U Non-Standalone (NR-U NSA) or LTE-LAA, overlooking challenges specific to NR-U Standalone (NR-U SA). These challenges include the absence of a licensed carrier for transmitting control signalling. Studies provided by vendors during the NR-U standardisation [10] use proprietary simulators, limiting result validation and replication, leaving a gap for open, verifiable research. Furthermore, a general challenge in NR-U SA or NSA that remains unaddressed in current literature is the implementation design of the Type 1 CAP which is an asynchronous CAP (i.e., load-based) into the NR-U system which inherits a synchronous, slot-based transmission framework. This will be further detailed in Section 4.2. Therefore, there is a pressing need for standard-compliant, open-source tools and methodologies to investigate and address the unique challenges of NR-U SA.

To address the research gaps outlined above, we focused on three key contributions:

- The first (to the best of our knowledge) standard-compliant NR-U SA simulation model for the ns-3 network simulator, which will be released as open-source upon publication.
- A novel scheduling technique for the Type 1 CAP called Scheduled Type 1 CAP
- An implementation of Additional Sensing (AS)
- Extensive system-level simulations analysing the coexistence of NR-U SA (testing different numerologies for variations of Type 1 CAP) and Wi-Fi at the sub-7 GHz bands, running eXtended Reality (XR) applications.

The proposed Scheduled Type 1 CAP seamlessly integrates the asynchronous Type 1 CAP, into the NR-U slot-based framework, which imposes a synchronous transmission constraint (transmissions can only start at the beginning of a slot boundary). This integration not only resolves compatibility issues with the NR-U framework but also enhances the validity of the sensing performed. Sensing the channel close to the transmission time decreases the likelihood of concurrent channel access with coexisting networks. However, due to the exponential random backoff used in Type 1 CAP, perfect alignment between the slot boundary and the completion of Scheduled Type 1 CAP is not always achievable. To address this misalignment issue, we propose using AS to prevent concurrent channel access with Wi-Fi networks or any coexisting networks. The proposed NR-U channel access enhancements can be extrapolated to coexistence scenarios with any legacy Wi-Fi devices due to their same CSMA/CA-based DCF procedure for channel access. Finally, we offer comprehensive insights into the synchronous and asynchronous LBT-based CAPs for sub-7 GHz as specified in 3GPP TS 37.213 [11]. We detail the design challenges and propose solutions for the NR-U Type 1 CAP. These challenges are particularly timely with the introduction of Type 1 Sidelink (SL) CAP in TS 37.213 Release 18 [11] Section 4.5, which adopts the NR-U Type 1 CAP and thus inherits the same issues. Our work addresses these shared challenges directly. The NR-U module we developed[1] will facilitate rigorous cross-layer evaluations and coexistence studies with other technologies. This advancement establishes a solid foundation for future research in this domain.

While this study focuses on inter-RAT coexistence between NR-U and Wi-Fi, we do not consider intra-RAT coexistence (e.g., NR-U/NR-U or Wi-Fi/Wi-Fi). Analysing intra-RAT coexistence would require a deeper investigation into aspects such as Wi-Fi signalling and its asynchronous transmission behaviour, which are beyond the scope of this work.

The structure of the paper is as follows: In Section 2, the related work in the field of coexistence in the shared spectrum is detailed. Section 3 presents the LBT procedures outlined in TS 37.213 [11]. Following this, Section 4 discusses the NR-U system design, challenges and the proposed solutions. In Section 5, we delve into the performance evaluation of various CAPs that have been described in Section 3 and implemented as described in Section 4. Finally, Section 6 discusses the key takeaways and outlines potential avenues for future research.

This paper uses several technical acronyms to describe the components and procedures involved in NR-U and Wi-Fi coexistence. For the reader's convenience, a list of acronyms and their definitions is provided in Table 1.

Table 1
List of acronyms.

Acronym	Definition
ACK	Acknowledgement
AS	Additional Sensing
BO	Buffer Occupancy
CAP	Channel Access Procedure
CAPC	Channel Access Priority Class
CWS	Contention Window Size
DCI	Downlink Control Information
HARQ	Hybrid Automatic Repeat Request
LBT	Listen-Before-Talk
MCOT	Maximum Channel Occupancy Time
NSA	Non-Standalone
RAT	Radio Access Technology
SA	Standalone
SCS	Subcarrier Spacing
UCI	Uplink Control Information

2. Related work

This section reviews key literature on CAPs for unlicensed spectrum in the sub-7 GHz. We begin by examining Frame-Based LBT (FB-LBT) studies, then transition to Load-Based LBT (LB-LBT), which is the core of our research and is referred to simply as LBT throughout the paper. We additionally discuss studies that rely on the obsolete Cat4 LBT and conclude with an overview of research gaps in existing approaches.

According to the 3GPP specifications, Frame-Based Equipment (FBE) employs a semi-static (synchronous) channel access procedure often referred to in the literature as FB-LBT. Conversely, Load-Based Equipment (LBE) uses a dynamic (asynchronous) LBT method. The

[1] https://gitlab.com/GeorgeFrangulea/ns3-nru-cap.

3GPP simply termed this as the CAP, while the research community may refer to it as LB-LBT or LBT.

In [25], a Markov model is presented to characterise the time-varying contention behaviour caused by bursty Machine Type Communication (MTC) in an LTE-LAA/Wi-Fi scenario where FB-LBT is used for channel access. The study shows that Time Division Multiple Access (TDMA) achieves overall throughput gains at the cost of centralised coordination. To address this, the authors propose a distributed approach that randomly spreads MTC access processes over the available time period, achieving performance comparable to TDMA. Authors in [26] describe an FB-LBT framework based on random walk theory, studying LTE-LAA/Wi-Fi coexistence. Their results reveal that while coexistence is feasible, Wi-Fi often dominates channel access due to the fixed frame periods where FB-LBT can be initiated. A dynamic approach to switching between FB-LBT and LB-LBT is analysed in [27], demonstrating that FB-LBT is particularly effective for devices with low-priority data or lower data arrival rates. In [28], the authors study a joint listening, probing, and transmission strategy for an FB-LBT system. The results show that the throughput-optimal strategy is to transmit whenever regulations permit. However, considering power consumption, the optimal strategy follows a pure threshold policy. An iterative algorithm with convergence analysis is used to compute the optimal threshold for channel access. A Markov model is employed in [29] to explore the limits of FB-LBT in LTE-LAA/Wi-Fi coexistence. The study shows that the LTE-LAA spectrum share exhibits a damped-oscillatory pattern as a function of the idle period, oscillating around the steady-state spectrum share. For idle periods significantly exceeding Wi-Fi transmission times, the oscillations diminish, and the steady-state and dynamic models converge. The work provides a formula to approximate the peak locations of the oscillatory pattern, enabling efficient tuning of the idle period to maximise LTE-LAA spectrum share, achieving up to 32% with 802.11n (20 MHz) and 46% with 802.11ac (160 MHz).

Several previous studies including Pei et al. [17,18,19], Zhou et al. [20], Wang et al. [21], Xiao et al. [22] and Parvini et al. [23] have recognised the significance of the LBT for cellular networks, such as LTE-LAA or NR-U to access a shared unlicensed channel. However, none of these studies implements the standardised Type 1 CAP [11], and instead, they rely on the non-compliant Cat4 LBT [3] which became obsolete in 2015. To address this, Sections 3.2 and 3.3 provide a clear explanation of TS 37.213 [11], which can be used to implement standard-compliant CAPs for LTE-LAA, NR-U networks and SL-U with the according parameters [30].

Other studies using the standard-compliant LBT have explored NR-U NSA or LTE-LAA Type 1 CAP coexistence with Wi-Fi. In [24] the analysis involved a simulation using ns-3, focusing on NR-U NSA that relies on a licensed carrier for control signalling and showing that Wi-Fi suffers degradation from inability to send critical control signalling. In [31], the authors used Markov Chain modelling to study LTE-LAA and Wi-Fi (LTE-LAA/Wi-Fi) coexistence when operating on multiple channels using multiple Channel Access Priority Classes (CAPCs). This work revealed that some of the channel access parameters defined by 3GPP lead to an unfair coexistence, degrading the Wi-Fi network performance. In both studies [24,31], the reliance on a licensed channel in NR-U NSA or LTE-LAA to transmit uplink (UL) control signalling bypasses fundamental issues associated with NR-U SA, such as intra-Radio Access Technology (RAT) LBT blocking due to Uplink Control Information (UCI) transmission. Consequently, these studies cannot be extrapolated completely onto the NR-U SA context.

Authors in [9] developed an analytical model to explore the use of multiple CAPCs within an NR-U network. They demonstrated that high-priority CAPCs can prevent low-priority CAPCs from accessing the channel. However, their abstracted model does not capture the synchronous transmission constraint in NR-U, where devices can only begin transmission at the start of a slot boundary. This omission is significant because the synchronous transmission constraint can exacerbate NR-U latency performance, as we discuss in Section 4.2. In [32] an analytical model was used to determine the optimal initial Contention Window Size (CWS) needed to maximise the throughput of an NR-U network while ensuring fairness to a coexisting Wi-Fi network. Despite these compelling results, their approach requires that the initial CWS of both NR-U and Wi-Fi be jointly tuned based on the number of nodes in both networks. However, this optimisation necessitates that the NR-U and Wi-Fi networks exchange information such as the number of active nodes. This is currently not feasible due to the absence of protocols or standards to support such inter-RAT communication.

The study in [33] uses a SimPy-based discrete-event simulator to evaluate ETSI LB-LBT [7] performance in NR-U gNB contention at sub-7 GHz bands. It examines gap-based and reservation signal (RS)-based channel access methods, highlighting a trade-off: gap-based access achieves higher channel efficiency and lower collision probability but faces fairness challenges, while RS-based access ensures fairness at the cost of reduced efficiency due to higher collision rates and wasted radio resources. Key findings include the importance of unsynchronised or offset slot boundaries to improve channel utilisation, the benefits of shorter synchronisation slots within allowable limits, and fairness enhancements through techniques like next transmission skipping. In [34], the authors evaluate the coexistence of random (Wi-Fi) and scheduled (LTE-LAA/NR-U) channel access in unlicensed bands, comparing gap- and RS-based methods for synchronous systems. It highlights that gap-based access avoids RS-related inefficiencies and interference, supports fair airtime sharing with Wi-Fi under short synchronisation slots, and reduces Wi-Fi collision probability compared to a Wi-Fi/Wi-Fi setup. However, synchronised scheduling among NR-U nodes is shown to cause starvation under high contention. A study detailed in [35] explores the LTE-LAA/Wi-Fi coexistence networks using a reservation-less gap mechanism. It demonstrates that treating gap periods as partial backoff preserves fairness without requiring reservation signals in 5G networks. Through analytical and simulation models validated on a testbed, the authors show how CW tuning can optimise coexistence for Downlink (DL) transmissions, achieving high per-node and per-cell fairness. However, for uplink transmissions, triggered uplink access on the Wi-Fi side, combined with CW tuning, is necessary to achieve a fair sharing of the spectrum. It should be noted that there is no clear consensus reached in the 3GPP RAN1 specification regarding the integration of RS, which is also known as blocking energy [36].

In [37] the authors describe the building blocks of CoBeam, a cognitive framework that enables spectrally efficient channel coexistence for heterogeneous networks. Results from a medium-scale testbed demonstrate that using specialised RF chains, Wi-Fi signals can be received and used to calculate a zero-forcing precoder. The precoder is then applied to the transmitted signal to reduce interference towards coexisting nodes. However, this implementation assumes that the received Wi-Fi signals do not fully overlap in the frequency domain with the primary network (e.g., NR-U) signals. If this condition is not met, channel estimation using a known standard-defined Physical Layer (PHY) preamble is not possible. Instead, blind or semi-blind channel estimation must be employed, which increases complexity [38]. In [30] the Type 1 CAP SL is evaluated for the SL-U, showing that the inherited NR-U synchronous transmission constraint leads to even higher degradation in SL-U networks due to the larger slot sizes. The authors in [39], emphasise the necessity for a broader range of studies incorporating diverse traffic types while underscoring the substantial influence of traffic load on the coexistence scenario.

In [40,41] a proprietary system-level simulator was used to gain insights into the NR-U framework. In [40], it was revealed that incorporating multiple switching points within the frame(i.e., switching from uplink (UL) to DL and vice versa) is beneficial at any traffic load level. It was shown that this approach significantly increases reliability and reduces NR-U latency by 38%. However, implementing multiple switching points within the slot comes at the cost of increased hardware complexity. Specifically, the Radio Frequency (RF) chains responsible for transmitting and receiving UL and DL signals must efficiently switch between modes. In [41], the authors evaluated a fully coordinated framework, demonstrating that UL LBT blocking (e.g., for UCI transmission) can be completely prevented. This approach assumes the possibility of synchronisation and coordination among NR-U base stations (as detailed in Section 3.2). Despite its enhanced reliability, this framework cannot be used when coexisting with Wi-Fi devices or any devices that operate based on an asynchronous CAP. In such scenarios, the Type 1 CAP must be used instead. Finally, a range of studies for indoor coexistence of NR-U/Wi-Fi at sub-7 GHz bands, employing a system-level simulator approach, are detailed in the NR-U standard [10] and are based on reports provided by various vendors such as Qualcomm [42], Ericsson [43], Samsung [44], and Nokia [45]. The overarching conclusion drawn from these studies was that Wi-Fi can coexist with NR-U. Notably, NR-U/Wi-Fi coexistence sometimes surpassed Wi-Fi/Wi-Fi coexistence due to Wi-Fi's lower Energy Detect (ED) threshold used when sensing non-Wi-Fi devices. In [43], Ericsson provided results showing NR-U latencies in the order of seconds, but no further insights were offered. Moreover, while these studies assume synchronised Next Generation Nodes B (gNBs), it remains unclear whether this synchronisation was employed to prevent packet collisions by ensuring the slot boundaries of different gNBs are not aligned.

In summary, while existing studies on NR-U and Wi-Fi coexistence have provided valuable insights, several research gaps remain. Many current studies rely on outdated, non-compliant Cat4 LBT, or they fail to fully address critical constraints of NR-U SA, or use proprietary simulations that limit transparency and reproducibility.

These research gaps highlight the necessity for a comprehensive, standard-compliant, and open-source simulator for studying the CAP for NR-U SA in coexistence scenarios with Wi-Fi. Our work addresses this challenge by developing a full-stack NR-U SA simulator aligned with the latest 3GPP standards. Additionally, we introduced a novel standard-compliant scheduling technique for the Type 1 CAP called Scheduled Type 1 CAP and implementation details for AS. This aims to allow a seamless integration for Type 1 CAP which is an asynchronous CAP, into the NR-U synchronous transmission and solve the misalignment problem and the associated degradation in latency and increased number of packets lost. This will enhance the compatibility of this procedure with the NR-U SA system. By doing so, we aim to provide a solid foundation for future research and facilitate rigorous evaluations of NR-U SA and future cellular-based technologies operating in the shared spectrum.

3. Shared spectrum channel access procedures in IEEE 802.11 and 3GPP NR-U

Efficient channel access is a cornerstone for the coexistence in shared spectrum environments. This section outlines the channel access procedures defined by 3GPP and IEEE standards, which form the foundation for NR-U and Wi-Fi coexistence. 3GPP TS 37.213 [11] provides specifications for the physical layer procedures used for channel access in shared spectrum. These procedures fall into two categories:

1. Asynchronous channel access that is load-based (defined simply as Downlink (DL) or Uplink (UL) CAPs).
2. Synchronous channel access that is semi-static (referred to as semi-static channel occupancy), also known as FB-LBT.

Asynchronous LBT is based on the CSMA/CA and can operate on different priorities similar to the IEEE 802.11 Enhanced Distributed Channel Access (EDCA) explained in Section 3.1. According to the 3GPP specification, the asynchronous LBT must be used when deploying cellular networks operating in the shared spectrum in areas where the level of regulation cannot guarantee the absence of Wi-Fi networks.

In scenarios where the absence of Wi-Fi can be reliably guaranteed, synchronous LBT can be implemented, which achieves a frequency reuse factor of 1 [11] and lowers channel access complexity by eliminating the need for random backoff. However, the synchronous LBT system requires precise time synchronisation of the gNBs. Synchronous LBT has the drawback of fixed delay overhead, as accessing the channel is only possible at certain intervals of time.

Table 2
EDCA channel access parameters.

AC A_i	d_i/T_{AIFS}	CW_{min}	CW_{max}	Max TXOP T_i [ms]
AC_VO	2/34 μs	4	8	2.08
AC_VI	2/34 μs	4	16	4.096
AC_BE	3/43 μs	16	1024	–
AC_BK	7/79 μs	16	1024	–

3.1. IEEE 802.11 enhanced distributed channel access

The IEEE 802.11 [5] standard supports multiple channel access schemes, with DCF and Enhanced-DCF (EDCA) being the most predominant. EDCA, on which our work also focuses, is based on CSMA/CA which operates as follows. An initiating node such as a Wi-Fi Access Point (AP) or Station (STA) using EDCA senses the channel for an Arbitration Inter-frame Space (AIFS) duration as indicated in Table 2. The backoff procedure can only start if the channel is sensed as idle during AIFS. During backoff, the channel is sensed for k sensing slots where k is randomly chosen from the range $\{0, \dots, W_j - 1\}$ where $W_j = \min\{2^j \cdot \mathrm{CW}_{\mathrm{min}}, \mathrm{CW}_{\mathrm{max}}\}$. Here, $\mathrm{CW}_{\mathrm{min}}$ represents the minimum contention window, $\mathrm{CW}_{\mathrm{max}}$ denotes the maximum contention window, and j signifies the retransmission attempt index. The initiating node must count down all k sensing slots as long as the channel remains idle. If the channel becomes busy during any k sensing slot, the initiating node must freeze the backoff counter until the channel becomes idle again. The channel must be idle for at least AIFS duration to resume the backoff procedure. If all k sensing slots are sensed as idle the initiating node can start transmitting for a duration that is less than or equal to its Transmit Opportunity (TXOP) set depending on the Access Categories (AC) used as indicated in Table 2. Once the TXOP duration has passed or the initiating node has released the channel, at the next channel acquisition the EDCA procedure updates parameter j used in calculating the CW based on the re-transmission attempt (e.g., CW is doubled if re-transmission is needed).

The EDCA was designed to enhance QoS provisioning by defining four ACs [31]. The configuration of the EDCA for each AC is shown in Table 2 as Voice (AC_VO), Video (AC_VI), Best Effort (AC_BE), and Background (AC_BK). Within a given Transmit Opportunity (TXOP) of an AC, a Wi-Fi node may transmit one or multiple MAC Service/Packet Data Units, each Acknowledged (ACK) by the responding node using a single Block ACK (BA). The initiating node signals the need for an ACK via a Block ACK Request (BAR) frame, prompting the responding node to issue the BA either immediately after the TXOP (immediate BA) or in subsequent TXOPs, thereby acknowledging multiple TXOPs with a delayed BA.

3.2. Semi-static channel occupancy

Due to the synchronous operation of FB-LBT, FBE nodes are allowed to utilise this CAP only in scenarios where LBE nodes (e.g., Wi-Fi) are absent on a long-term basis (e.g., due to regulatory constraints). Consequently, FB-LBT is primarily envisioned for use in controlled unlicensed environments, such as 5G/6G private networks, industrial settings, or indoor deployments. For such scenarios where the FBE gNBs are centrally coordinated it has been identified in [41] and Section 7.2.1.1 [10] that LBT failure is negligible.

Given the standalone and synchronised nature of FB-LBT, for Industrial Internet of Things (IIoT) implementation and Ultra-Reliable Low Latency Communications (URLLC) for private networks in the shared

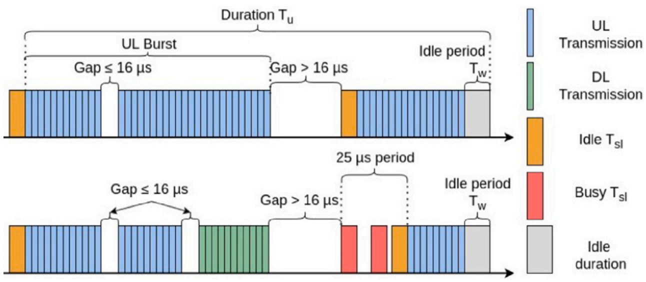

Fig. 1. UE-initiated semi-static channel occupancy according to 3GPP TS 37.213.

spectrum in, the procedure was extended to allow User Equipment (UE) channel acquisition if indicated by the serving gNB [11]. The gNB configures in all UEs within its serving cell a parameter, T_x, to indicate the periodicity of the Channel Occupancy Time (COT) in milliseconds (ms). The Maximum Channel Occupancy Time (MCOT) must be $T_y = 0.95T_x$. At the end of each COT, the gNB must introduce an idle period known as T_z defined as $max(0.05T_x, 100\ \mu s)$. The gNB can instruct the UEs under its control to initiate a COT. Such configuration involves a unique ue_{period} and ue_{Offset}, so the UE can then initiate a channel occupancy on a channel(s) within the bandwidth of the serving cell with a periodicity $T_u = ue_{Period}$ in ms with a maximum COT of $T_v = 0.95 \cdot T_u$. The $T_o = ue_{Offset}$ represents the number of symbols from the beginning of the synchronised radio frame to the start of the first period where the UE can initiate a channel occupancy. The idle period for UE is denoted as $T_w = max(0.05T_u, 100\ \mu s)$. The UE can be an initiating node for a given channel only if it knows the gNB COT by detecting a first DL transmission within a frame or through a DCI indication.

In Fig. 1, the UL and DL transmission of a UE and gNB, respectively, are illustrated for a semi-static channel occupancy initiated by the UE. The UE can initiate a channel occupancy in a period of duration T_u and transmit at the start of the period T_u right after the channel is sensed to be idle for $T_{sl} = 9\ \mu s$, and must finish transmission before the start of the idle period. The UE-initiated COT procedure must only occur if the UE's transmission buffers are non-empty so that data transmission can begin at the start of the COT. Fig. 1 illustrates the conditions in which UL or DL transmission(s) are allowed in a COT initiated by the UE, which are described as follows:

- Any transmission within the MCOT ends before the idle duration.
- For cases where the gap between the UL transmission and any previous transmissions is larger than 16 µs, the channel must be sensed idle for a sensing slot duration $T_{sl} = 9\ \mu s$. No sensing is required for gaps smaller than 16 µs.
- If the gap between DL and a previous UL transmission is more than 16 µs, then the channel must be sensed idle for at least a $T_{sl} = 9\ \mu s$ within a 25 µs interval ending right before the intended DL transmission. No sensing is required for gaps smaller than 16 µs.

3.3. Channel access procedures for downlink and uplink

This section will introduce the transmission requirements for each DL/UL CAP from TS 37.213 Release 18 [11] for NR-U. The discussion for Type 1 CAP based on Fig. 2 is also applicable to SL-U, however, Table 3 will have SL-U specific parameters.

3.3.1. Type 1 channel access procedure

Type 1 CAP implements an exponential random backoff and is the primary LBT procedure for channel acquisition in the shared spectrum. It is employed in cases where the time duration spanned by the sensing slots over which the channel must be sensed as idle is random. According to TS 37.213 Release 18 [11], Fig. 2 illustrates the flow diagram of the Type 1 CAP while Table 3(a) and 3(b) show the configurations that the procedure can be set with to achieve a different level of priority for UL or DL transmission respectively. The CAPCs for Type 1 UL CAP are designed to be more stringent when allowing devices to access the channel by imposing longer sensing durations. In Fig. 2, the option of permitting a transmission after sensing the channel idle during a defer duration T_d, as detailed in Cat4 LBT in TR 36.889 [3] but removed in TS 37.213 [11], is highlighted in red. For this work, we have introduced the possibility to activate or deactivate this option, allowing to seamlessly switch between Cat4 (Rel13) LBT (that does not require a mandatory backoff) and Type 1 CAP (which requires a mandatory backoff). Cat4 LBT was left as an option in our work solely for analysis purposes, to demonstrate the degradation it can cause to coexisting networks when the non-compliant procedure is used. The green highlighted region indicates the procedures implemented in this work, in which the procedures from [11] were incorporated as well as the proposed implementation of AS. Including the updated procedures was necessary because the previous version of the NR-U model was based on the Cat4 LBT.

Table 3
Channel Access Priority Class (CAPC) for (a) UL and (b) DL.

(a)

CAPC (p)	m_p	$CW_{min,p}$	$CW_{max,p}$	$T_{mcot,p}$ [ms]	Allowed CW_p sizes
1	2	3	7	2	{3,7}
2	2	7	15	4	{7,15}
3	3	15	1023	6 or 10	{15,31,63,127,511,1023}
4	7	15	1023	6 or 10	{15,31,63,127,511,1023}

(b)

CAPC (p)	m_p	$CW_{min,p}$	$CW_{max,p}$	$T_{mcot,p}$ [ms]	Allowed CW_p sizes
1	1	3	7	2	{3,7}
2	1	7	15	3	{7,15}
3	3	15	63	8 or 10	{15,31,63}
4	7	15	1023	8 or 10	{15,31,63,127,511,1023}

Given that a transmission has been initiated using the Type 1 CAP set with a given CAPC denoted as p, as shown in Fig. 2, the initiating node will first sense the channel for a defer duration T_d, where this duration takes the same values as AIFS in the Wi-Fi EDCA procedure. This is done to ensure equal opportunity to access the channel. The defer duration is defined as $T_d = T_f + m_p \times T_{sl}$, where T_f is equal to 16 µs and encompasses a sensing slot, T_{sl} at the beginning, and m_p depends on the CAPC used and the direction of transmission (see Table 3(a) and 3(b), for UL and DL, respectively). The defer duration is deemed idle if all sensing slots (all T_{sl} within T_f) are idle, i.e., energy sensed is below the ED threshold (X_{Thresh}) for at least 4 µs within a T_{sl}. Considering the channel was sensed as idle during the duration T_d, CW_p is set to its minimum value, $CW_{\min,p}$. Fig. 2 shows that in step 1, the counter N is randomly chosen from the range $[0, \ldots, CW_p]$, which is followed by step 4. If the counter is randomly chosen to be 0 and the initiating node has packets in the queue, it can access the channel for a specified MCOT. However, if the counter is greater than 0, step 2 is executed, where the counter N is decremented (if the initiating node chooses to do so). Step 3 involves sensing the channel for a duration of T_{sl}. If T_{sl} is idle, the counter is rechecked in step 4. If the channel is busy, the procedure enters a loop consisting of steps 5 and 6, repeatedly sensing the channel for an additional duration of T_d until the channel becomes idle and the procedure can resume. Assuming that the counter N is decremented to 0 successfully and that the initiating node did not initiate a transmission due to an empty transmission queue or misalignment with the slot boundary, we propose implementing an Additional Sensing (AS). The implementation of the AS is our proposed interpretation of the definition of Type 1 CAP from TS 37.213 [11] since the case of misalignment with the slot boundary is not specifically

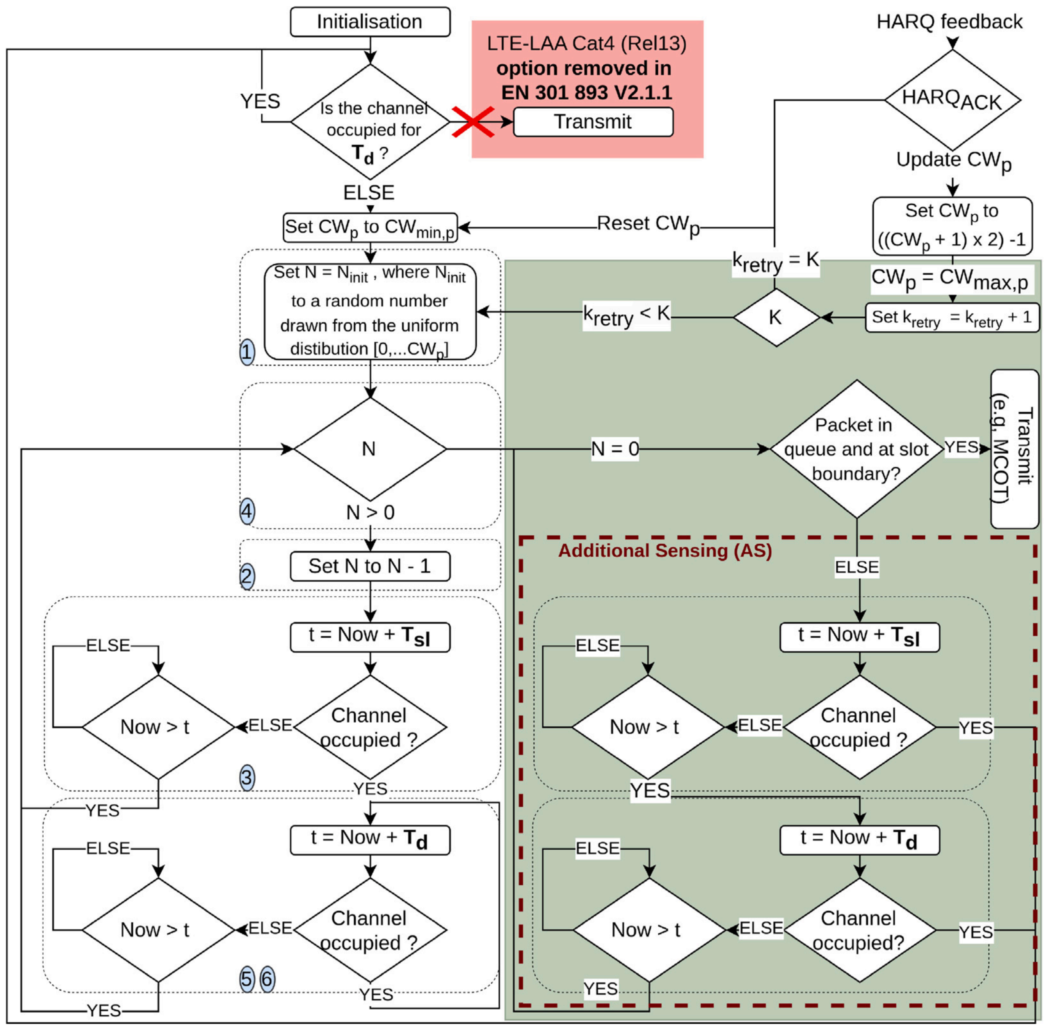

Fig. 2. Type 1 CAP algorithm based on the TS 37.213 Section 4.1.1. with additional sensing.

defined. In the AS phase depicted in Fig. 2, the initiating node must sense the channel as idle during all sensing slots within the combined duration of a T_{sl} sensing slot and a T_d in order to have another attempt to start a transmission. Otherwise, the Type 1 CAP is re-initialised.

Upon successful initiation of a COT by the initiating node and availability of Hybrid Automatic Repeat Request (HARQ) feedback, the CW_p will be adjusted as illustrated in Fig. 2. For cases where transport block-based feedback is employed, the CW_p is reset to $CW_{\min,p}$ if at least one HARQ-ACK feedback is an ACK, while if code block group-based feedback is employed, at least 10% of the HARQ feedback must be ACKs. In all other cases, the CW_p will be increased to the next higher allowed value. If CW_p has already reached the maximum allowed value for that particular CAPC, it will either remain at the maximum value or be reset to $CW_{min,p}$ based on the value of the parameter k set by the initiating node [11]. The parameter k can take values within the $\{1, 2, \dots, 8\}$ range and determines how many consecutive times $CW_p = CW_{\max,p}$ can be used for a given CAPC p.

3.3.2. Type 2 channel access procedure

Type 2 CAP has three subcategories used in cases where the time duration spanned by the sensing slots over which the channel must be sensed as idle is deterministic.

The first subcategory, Type 2A, is implemented for scenarios where a channel must be acquired for transmissions containing discovery bursts only or discovery bursts multiplexed with non-unicast data. It is also used in Sidelink Synchronisation Signal Block (S-SSB) transmissions, where the duration is at most 1 ms and the discovery burst duty cycle is at most 1/20. Additionally, Type 2A applies to transmissions on a shared channel occupancy (acquired using Type 1 CAP) of a gNB or UE that follows a UL or DL transmission after a gap of at least 25 μs. Type 2A CAP is deemed successful if the channel remains idle during a sensing interval of $T_{short_{dl}} = 25$ μs, where $T_{short_{dl}}$ comprises a 16 μs duration (T_f) with one sensing slot T_{sl} at the beginning of the sensing interval, immediately followed by another sensing slot. The interval $T_{short_{dl}}$ is deemed idle if both sensing slots are idle. The same applies for $T_{short_{ul}}$ for the equivalent procedure in the UL (at the UE side).

Type 2B CAP should be used for transmissions on a shared channel occupancy (acquired using Type 1 CAP) of a gNB or UE that follows a UL or DL transmission, respectively, after a gap of 16 μs. Type 2B CAP is considered successful if the channel is sensed idle within a duration of $T_f = 16$ μs, where T_f includes a sensing slot within the last 9 μs of T_f. The duration of T_f is deemed idle if the channel is sensed idle for at least 5 μs, where at least 4 μs of sensing occurs within the sensing slot.

Type 2C is used in a shared channel occupancy (acquired using Type 1 CAP) where the gap between current and previous transmission is less than 16 μs, and the transmission has a maximum duration of 584 μs. Type 2C is used for immediate transmission, and it requires no sensing.

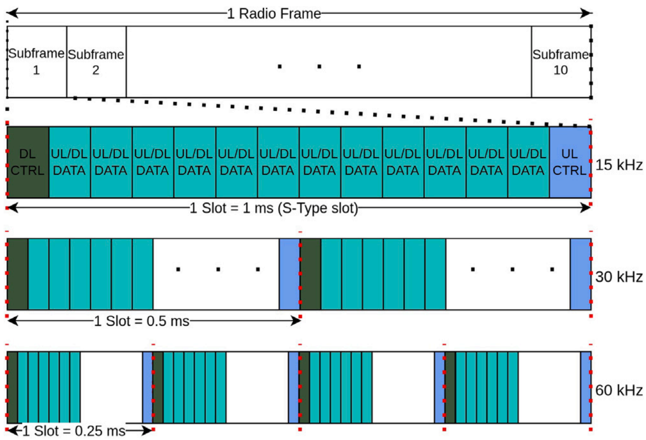

Fig. 3. 5G NR radio frame structure and slot configuration used for this work, i.e., all S type slots, and numerology 0, 1, and 2.

4. NR-U system model, design challenges and solutions

To evaluate the coexistence of NR-U and Wi-Fi in shared spectrum scenarios, we use and extend the ns-3 5G-LENA module. This tool provides a comprehensive simulation environment for studying the interactions between these technologies. The ns-3 5G-LENA is a discrete-event simulator that includes a full-stack implementation featuring a 3GPP standard-compliant NR module for PHY and MAC layers and upper layers [46]. The high-fidelity protocol stack enables rigorous cross-layer evaluations and facilitates interoperability studies with other technologies, such as Wi-Fi. The NR module has been rigorously calibrated for indoor and outdoor environments to ensure consistency with real-world deployments and propagation conditions specified by 3GPP [47]. Our research aims to comprehensively evaluate NR-U standalone performance, built upon the NR module, from application-level interactions to the PHY layer. The NR module provides a range of NR-U functionalities, such as distinct Channel Access Manager (CAM) implementations. Crucial NR-U supporting features like energy detection, COT sharing, and the unlicensed mode PHY state machine are seamlessly integrated into the core NR module library.

4.1. NR-U system model

Fig. 3 shows the NR frame with an S-type slot configuration for sub-7 GHz SCS of 15, 30, and 60 kHz. The NR module implements the NR Time Division Duplexing (TDD) pattern scheduling, allowing the configuration of a specific TDD pattern in compliance with 3GPP standards [48]. The S-type slot used in this study consists of a DL and UL symbol at the beginning and end of the slot, respectively, to transmit Downlink Control Information (DCI) and UCI. The rest of the 12 OFDM symbols are flexible (F) symbols and can be used for UL or DL data transmissions. An important aspect when choosing the SCS used is each numerology flexibility. The SCS is inversely proportional to the duration of each Orthogonal Frequency Division Multiplexing (OFDM) symbol. This means that a higher SCS results in shorter transmission times. However, a higher SCS also leads to decreased Resource Block (RB) size, which can be crucial in high-interference scenarios. With larger Transmission Block (TB) sizes, the error probability is lower, so increasing the SCS can lead to a higher probability of error.

Fig. 4 illustrates the architecture of the system model of the NR-U standalone device. The system includes a Component Carrier Manager (CCM), which oversees traffic distribution across multiple carriers. A Channel Access Manager (CAM) determines how the NR-U device accesses the channel for each carrier. The gNB CAM implements Type 1 and 2 CAP, while UE CAM can only access the gNB channel through a

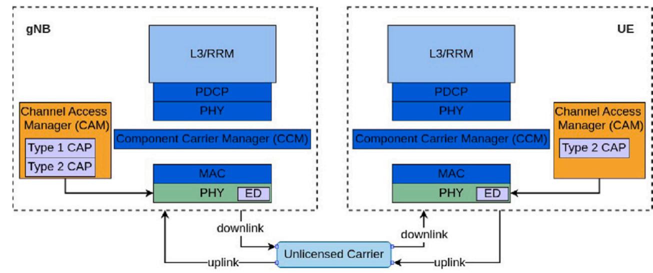

Fig. 4. NR-U standalone system model.

Type 2 CAP. The option of allowing transmission after a defer duration (shown as initial CCA in Section 7.2.1.6 Fig. 7.2.1.6-1 [3]) was removed (i.e., not implemented) for Type 1 CAP. The option to deactivate or activate the mandatory backoff was implemented, allowing the switch between Cat4 (Rel13) and Type 1 CAP. The NR-U model incorporates sensing capabilities through an ED mechanism at the PHY layer, which performs channel sensing based on signals from the CAP blocks in the CAM. The primary goal is to verify channel availability before initiating transmission.

4.2. Design challenges and proposed solutions

Type 1 CAP is an asynchronous (i.e., load-based) procedure designed by 3GPP to adhere to ETSI regulations [7]. This procedure is aligned with the Wi-Fi 802.11 CSMA/CA-based DCF procedure, which operates asynchronously (i.e., Wi-Fi can start transmitting at any time). However, NR-U systems inherit a synchronous, slot-based framework, constraining transmissions to begin only at slot boundaries. This discrepancy leads to synchronisation gaps (i.e., time durations between the completion of Type 1 CAP and the next slot boundary) during which the gNB must wait idly before initiating transmission. Synchronisation gaps introduce several challenges that negatively impact NR-U performance and coexistence with Wi-Fi networks:

- Invalid sensing results: as synchronisation gaps increase, the initial sensing becomes less reliable. Coexisting Wi-Fi can start transmitting within those gaps leading to packet collisions.
- Higher latency: synchronisation gaps introduce additional delays before data transmission can commence, which is detrimental for latency-sensitive applications in NR-U.

To directly address the synchronisation gap and misalignment issues, we propose two solutions compliant with TS 37.213 [11]:

- Scheduled Type 1 CAP: We introduce a scheduling technique that leverages existing information at the gNB's physical (PHY) layer without adding network management complexity. By scheduling the Type 1 CAP closer to the intended transmission slot, we enhance the validity of the sensing performed during backoff and reduce latency. This approach is feasible because the NR module assumes a default 2-slot delay for MAC-to-PHY processing [4], allowing the MAC layer to anticipate data scheduled for upcoming slots.
- Additional Sensing (AS): Since perfect alignment between the completion of Type 1 CAP and the slot boundary cannot always be guaranteed due to random backoff, AS is implemented. The integration of AS ensures that the misalignment does not lead to concurrent transmissions with coexisting networks. The AS is performed right before the slot boundary if data is ready for transmission.

Fig. 5 depicts an NR-U transmission at an SCS of 15 kHz on a channel acquired via Scheduled Type 1 CAP set with priority (i.e., CAPC) p1 where the channel is shared through Type 2 CAP and (a) with

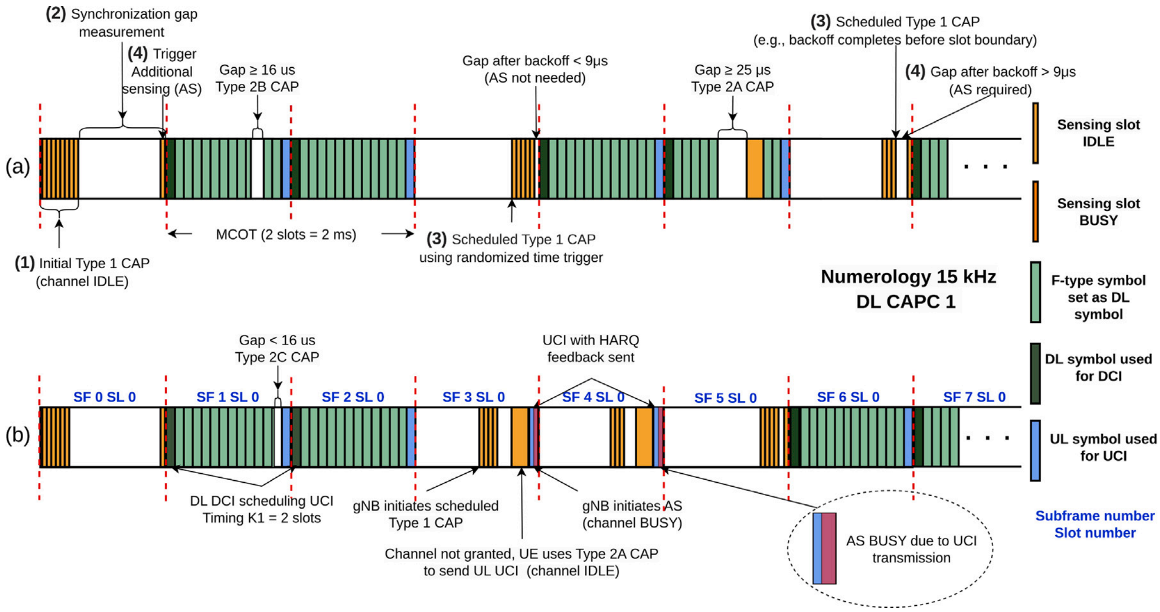

Fig. 5. NR-U Scheduled Type 1 CAP channel access and Type 2 CAP for COT sharing, SCS 15 kHz, CAPC 1 for (a) HARQ-feedback disabled and (b) HARQ-feedback enabled.

HARQ-feedback disabled and (b) with HARQ-feedback enabled. Using Fig. 5(a), the Scheduled Type 1 CAP with AS can be described as follows:

1. Initial Type 1 CAP: The gNB performs the Type 1 CAP at the start of the slot boundary to acquire the channel for the first transmission.
2. Synchronisation gap measurement: After step 1, the gNB measures the synchronisation gap between the completion of the Type 1 CAP and the slot boundary.
3. Randomised triggering of Scheduled Type 1 CAP: A random time value between 90% and 100% of the measured synchronisation gap is calculated and used to trigger Scheduled Type 1 CAP. Randomising the start of Scheduled Type 1 CAP aims to mitigate the synchronisation of the backoff amongst different gNBs which can lead to throughput degradation [30].
4. Additional Sensing (AS): If alignment is not achieved, AS is used before transmission to check the channel availability. Alignment is considered true if the time between the end of backoff and the next slot boundary is less than one sensing slot (i.e., $T_{sl} = 9$ μs).

Please note that steps 1 and 2 above must be repeated if the gNB changes the slot structure, as the synchronisation gap can vary from 0.25 ms to 1 ms depending on the SCS used.

Once the gNB acquires the channel the Scheduled Type 1 CAP, the transmission starts according to the S-type slot format, and the MCOT is shared using Type 2 CAP. The specific Type 2 CAP used (Type 2A, 2B, or 2C) depends on the gaps between the gNB DL transmission and the UE UL transmission, which can have durations of less than 16 μs, between 16 μs and 25 μs, or greater than 25 μs, respectively.

Fig. 5(b) illustrates a drawback of NR-U SA when HARQ feedback is used. Using a licensed carrier for critical signalling mitigates the issue we describe next. While using a licensed carrier for critical signalling (e.g., LTE-LAA or NR-U NSA) can prevent this issue, it is not an option in the NR-U SA context. Under the current NR-U specification, it is impossible to guarantee that HARQ feedback is sent within the MCOT. This problem arises because the MCOT duration may expire before the feedback can be sent, or the gNB must release the channel upon failure of a Type 2 CAP. This limitation also explains why results from NR-U NSA or LTE-LAA are not directly applicable to the NR-U SA context. If the MCOT is reached and the UE has not sent the HARQ feedback, the UE must initiate a Type 2A CAP to check channel availability and transmit the UL UCI containing the HARQ feedback. Such occurrences are highly likely to block the gNB from accessing the channel.

In Fig. 5(b) this issue is depicted, where, in the DL DCI of SF1 SL 0 and SF 2 SL 0, the K1 parameter is sent to the UE to indicate where the UL UCI containing HARQ feedback must be sent. In this case, the UE will have to use the last symbol in the slot, which is always UL, for the S-type slots. Based on K1, in this case, the HARQ feedback must be sent with an offset of 3 slots. The K1 parameters can vary from 1 to 4 slots. Fig. 5(b) depicts the case where MCOT has been reached at the end of SF 2 SL 0. Since the UE is expected to send HARQ feedback in SF 3 SL 0 and SF4 SL 0, but the channel is not granted, it must use a Type 2A CAP. After the end of MCOT, due to existing scheduling, the gNB schedule Type 1 CAP in SF 3 SL 0. The channel is sensed as idle during the backoff, and AS is scheduled before the next slot boundary. The lack of transmission on the channel also allows the UE Type 2A to be completed, thus allowing transmission of the HARQ feedback within the last symbol of the slot. The transmission of the HARQ feedback will block the UE's serving gNB from completing the AS, which will then have to restart Type 1 CAP in SF 4 SL 0. In the example depicted in Fig. 5(b), HARQ transmission is scheduled in consecutive slots SF 3 SL 0 and SF 4 SL 0, leading to recurrent blocking of the gNB during AS.

5. Performance evaluation

This section evaluates the proposed Scheduled Type 1 CAP and its variations in coexistence scenarios with Wi-Fi, focusing on their impact on key performance metrics such as packet loss, latency, and throughput. This study focuses on isolated inter-RAT coexistence between NR-U and Wi-Fi, specifically analysing how the CAP design impacts NR-U performance and coexistence with Wi-Fi.

To validate the proposed Scheduled Type 1 CAP, we test four variations, including Cat4 (Rel13). Specifically:

- *Cat4 Rel13*: Category 4 LBT as per TS 36.889 Release 13 [3].
- *Scheduled Type 1 CAP (no AS)*: This CAP uses the scheduling technique and does not implement the AS.
- *Scheduled Type 1 CAP*: This is the Type 1 CAP as per TS 37.213 [11] using the proposed scheduling technique and AS.

The Type 1 CAP (no AS, no scheduling), which only includes the mandatory backoff, was also tested and showed marginal improvements over Cat4 Rel13. To maintain clarity and avoid overcrowding the analysis, this dataset has been excluded and is available in the repository for this study[1].

5.1. NR-U and Wi-Fi evaluation campaign

This subsection presents a simulation campaign to evaluate how different CAPs (priority p2 or p4) affect NR-U operating at SCS values of 15, 30, and 60 kHz in coexistence with Wi-Fi 6, also known as 802.11ax. Specifically, NR-U CAP set with p2 is tested alongside Wi-Fi 6 EDCA set to AC_VI, while NR-U with p4 is tested with Wi-Fi 6 EDCA set to AC_BE. We modelled the system according to Table 4, aiming for a high load (BO > 55% [42]). To evaluate the performance of the CAP, each UE/STA was assigned a single DL flow of XR-type traffic, specifically Cloud Gaming (CG) [49,50]. This traffic is characterised by a fixed data rate of 20 Megabits/second and a frame generation rate of 60 frames per second (FPS). The data were collected over 79 independent simulation runs. In each simulation, the application duration was set to 10 s, resulting in 600 packets being sent, with an average packet length of 41 700 bytes. The collected data is visualised as Cumulative Distribution Functions (CDFs) plotted for each SCS.

An important aspect to consider in this analysis is the priorities set for the tested NR-U CAP and Wi-Fi EDCA, namely:

- When NR-U CAP is set with priority p2, the Wi-Fi EDCA is configured with AC_VI. Both settings are designed for high-priority traffic, such as video streaming, and are characterised by a low maximum CWS of 15, which can result in up to 0.135 ms of sensing duration. The main difference is that Wi-Fi AC_VI allows for an MCOT of 4.096 ms while NR-U CAP set with priority p2 allows for an MCOT of 3 ms.
- When NR-U CAP is set with priority p4, the Wi-Fi EDCA is configured with AC_BE. Both settings are designed for best-effort traffic and are characterised by a high maximum CWS of 1023, which can result in up to 9.207 ms of sensing. The main difference is that Wi-Fi AC_BE allows for an MCOT of 5.484 ms while NR-U CAP set with priority p4 allows for an MCOT of 8 ms.

Table 4
Scenario configuration parameters.

Parameter	Value
System-level simulator	
ns-3, simulator release	Release ns-3.40
5G-LENA NR module	Release v2.6.y
Independent runs	79 repetitions per setup (RNG values 1–79)
Simulation time	12 s
Deployment and propagation parameters	
Channel model	3GPP InH mixed office model
Deployment scenario	Indoor-B (small InH office model)
Channel bandwidth	20 MHz
Central frequency	5.22 GHz
Traffic parameters	
Direction	Downlink
Traffic type	Cloud gaming (R:20 Mbps, Fps:60)
Device parameters	
gNB/AP; UE/STA Antennas	2 × 2; 1 × 2
gNB/AP; UE/STA Tx Power	24 dBm; 18 dBm
gNB/AP Noise figure	5 dB
UE/STA Noise figure	9 dB
NR-U/Wi-Fi Transmission	Quasi-omnidirectional
NR-U parameters	
Frame structure	SCS of 15, 30 and 60 kHz
Control/data symbols	2/12 symbols
Scheduling	proportional fair
CAP ED	−72 dBm
Channel access priority class	*p2* or *p4*
Modulation and coding scheme	MCS Table 2
HARQ combining method	Incremental redundancy
Max. no. of HARQ processes	20
Max. no. of HARQ retransmissions	3
UE processing delay (K1)	2 slots
RLC mode	Unacknowledged mode
Wi-Fi parameters	
A-MPDU	9000 bytes
Guard interval	1.6 μs
Access category	*AC_VI* or *AC_BE*
CCA CS/ED	−82 dBm/−62 dBm

5.2. Network topology

The 3GPP Indoor-B model [51] was employed as a deployment scenario, featuring one base station and two users per network NR-U and WI-FI network. This model was adjusted to reflect realistic sub-7 GHz network deployments, resulting in an office layout measuring 40 m by 40 m. Each operator's base station was positioned at a height of 3 m. Base stations were uniformly randomly distributed within a virtual 10-m by 10-m box, ensuring a minimum separation distance of 2 m between each operator's base station. Users were uniformly randomly distributed within the office space, positioned at a height of 1 m.

5.3. Impact of NR-U numerology

For the remainder of this section, we group Cat4 (Rel13), and Scheduled Type 1 CAP (no AS) as *CAPs without AS*. We also include our proposed Scheduled Type 1 CAP (which uses AS), triggered by the scheduling technique described in Section 3.3.

5.3.1. Transport block and MAC protocol data unit loss

Fig. 6(a), (b), and (c) present the distribution of TB losses in NR-U for SCS values of 15, 30, and 60 kHz, respectively. We gathered these statistics at the PHY layer via the New Data Indicator (NDI), which flags new data transmissions. Under ideal Signal-to-Interference-plus-Noise Ratio (SINR) conditions and employing a Modulation and Coding Scheme (MCS) of 27, the TB sizes are approximately 12,976 bytes, 6488 bytes, and 3182 bytes for an SCS of 15 kHz, 30 kHz, and 60 kHz, respectively. Consequently, transmitting a single packet of approximately 41 700 bytes requires approximately 4, 7.7, and 15.7 TBs. An increased number of lost TBs may indicate the failure of the CAP to prevent concurrent channel access with the coexisting Wi-Fi network.

First, we examine the Scheduled Type 1 CAP. In Fig. 6(a), (b) and (c) both priority p2 and p4 exhibit the lowest TB loss across all SCSs and do not show an exponential increase in TB loss. This indicates the efficacy of the AS used by these CAPs in preventing concurrent channel access. The minimal difference between the two priorities suggests that the larger CWS has only a marginal effect on preventing interference when AS is used.

In contrast, for the CAPs without AS, an exponential increase in TB loss is observed across all SCSs for both priorities. These findings suggest that concurrent channel access frequently occurs, particularly for priority p2, which shows the highest rate of packet collisions. This is in part due to the priority p2's smaller MCOT, which requires the gNB to re-lease and re-acquire the channel more frequently. It is also evident that the larger CWS associated with priority p4 results in a lower number of lost TBs as the larger CWS leads to fewer channel access opportunities. For priority p2, the scheduled Type 1 (no AS) is the only procedure that achieves a performance that is comparable to that of priority p4. This indicates that even with a considerably smaller CWS, scheduling the backoff closer in time to the transmission allows for a better channel assessment, thereby deferring the transmission.

Fig. 7(a), (b), and (c) present the number of lost Wi-Fi MAC Protocol Data Units (MPDUs) observed when the NR-U employs different CAPs

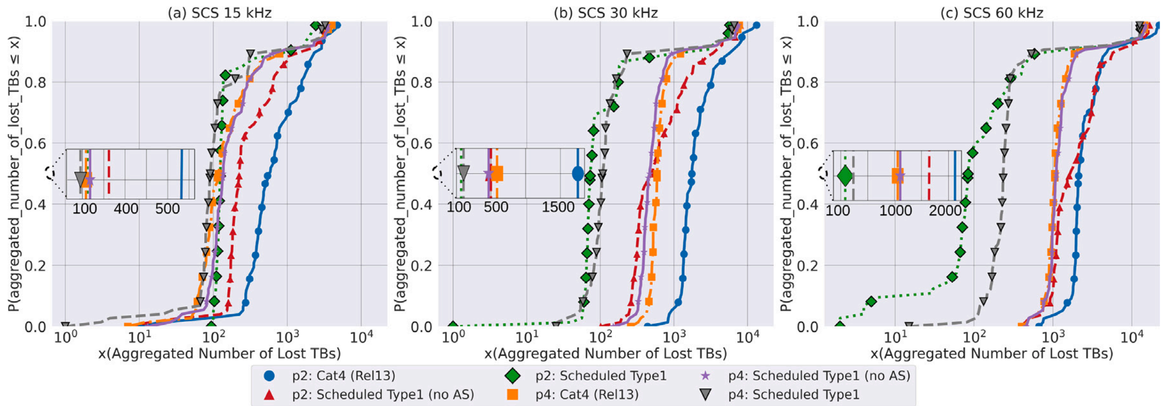

Fig. 6. Aggregated TB loss at NR-U for various CAPs set with priority *p2* or *p4* evaluated at: (a) SCS 15 kHz, (b) SCS 30 kHz and (c) SCS 60 kHz, in coexistence with Wi-Fi 6.

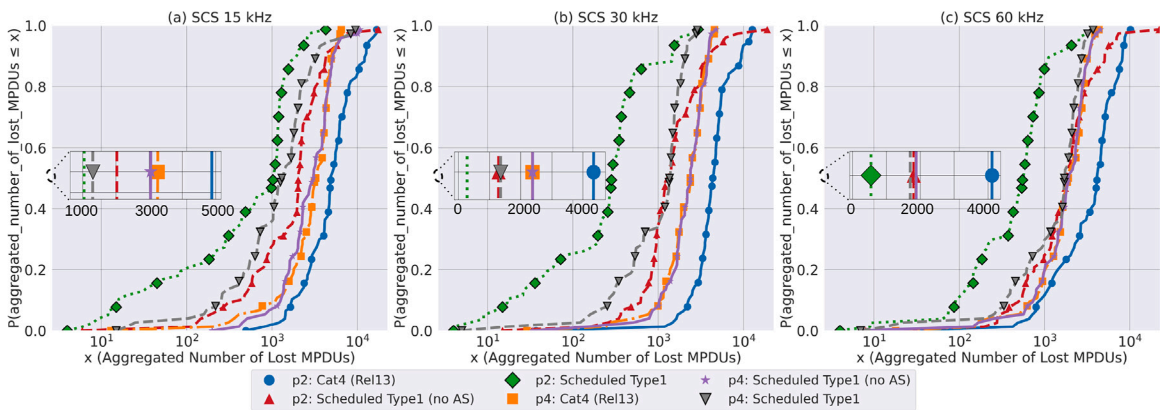

Fig. 7. Aggregated MPDU loss at Wi-Fi 6 when coexisting with NR-U utilising various CAPs set with priority *p2* or *p4* at: (a) SCS 15 kHz, (b) SCS 30 kHz and (c) SCS 60 kHz.

and priorities with SCSs of 15, 30, and 60 kHz, respectively. Note that the Wi-Fi 802.11ax SCS is constant at 78.125 kHz. Consequently, the number of MPDUs across which packets are fragmented is also constant for a given MCS and SINR. The Aggregated-MPDU (A-MPDU) was set to 9000 bytes for a payload duration of 0.608 ms (8 aggregated MPDUs of 1038 bytes each). The lowest number of lost MPDUs is observed when NR-U employs Scheduled Type 1 CAP, with the CAP set to priority p2 achieving the best performance. This indicates that for priority p2, where the NR-U MCOT is 3 ms compared to Wi-Fi's AC_VI MCOT of 4 ms, fewer MPDUs are lost. Therefore, when the two coexisting networks use an MCOT of similar duration, the result is improved coexistence, allowing the Wi-Fi network to send its data more efficiently.

For NR-U CAPs without AS, Wi-Fi experiences a decreasing number of lost MPDUs as SCS increases, which is more pronounced for priority p4. The increased number of lost TBs at higher SCS values in NR-U causes more frequent received NACKs leading to doubling the CWS. The use of larger CWS, which in turn raises the likelihood of channel access failure, which allows the Wi-Fi network to transmit. Amongst the CAPs without AS, the CAPs that use the scheduling technique are shown to lead to a lower number of lost MPDUs. This indicates that even in the absence of AS, scheduling the backoff closer to the start of the transmission prevents some instances of concurrent access with Wi-Fi devices.

5.3.2. *Backoff occupancy and buffer occupancy*

Fig. 8 illustrates two key metrics that capture how intensively the NR-U gNB contends for and occupies the channel:

- Backoff occupancy, denoting the fraction of simulation time spent in backoff due to the LBT-based CAP. This metric excludes any time spent on AS, synchronisation gaps, and additional backoff periods following an AS failure.
- Buffer occupancy (BO), defined as the percentage of simulation time during which the Radio Link Control (RLC) transmission buffers are non-empty.

In Fig. 8, the blue bars represent backoff occupancy while the orange bars represent BO. Fig. 8(a), (b), and (c) correspond to SCS values of 15, 30, and 60 kHz, respectively, and each bar group (black or grey outlines) represents a specific CAP priority (p2 or p4).

Across all CAPs tested, the results show that backoff occupancy increases with higher SCS. The primary cause is the larger number of lost TBs at higher SCS values, which necessitate more frequent channel acquisitions for retransmissions. Among the evaluated CAPs, Scheduled Type 1 exhibits the lowest backoff occupancy, owing to its lower rate of lost TBs; fewer failed transmissions reduce the number of Type 1 CAP initialisations. Notably, assigning p4 to Scheduled Type 1 yields the lowest backoff occupancy overall, indicating that the wider MCOT and larger CWS of p4 improve efficiency when AS is in use. In contrast, CAPs assigned p2 show higher backoff occupancy, primarily because the shorter MCOT of 3 ms requires frequent channel re-acquisition, thereby increasing the time spent in backoff.

Regarding BO, the right-hand orange bars in each group of Fig. 8(a) (b) and (c) show that the priority level associated with each CAP significantly impacts BO. Following the ranges defined in [42], BO values of 10% to 25% indicate low load, 35% to 50% indicate medium load, and values above 55% indicate high load. Higher SCS is associated with shorter slot duration, enabling more frequent channel access and faster servicing of RLC buffers. However, the stricter slot-aligned channel access of NR-U, combined with shorter MCOT for p2, can introduce delays. In Scheduled Type 1 CAP, the stringent sensing

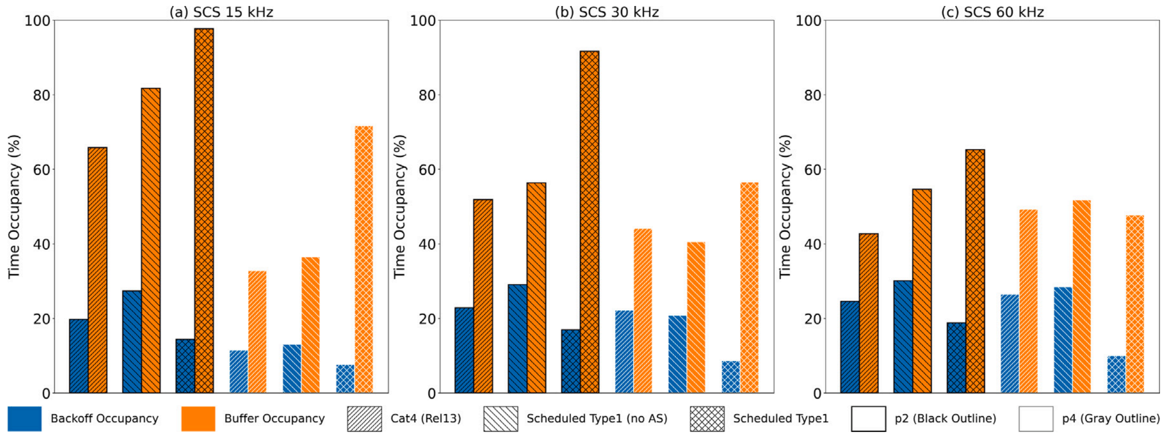

Fig. 8. Backoff and Buffer Occupancy for NR-U when coexisting with Wi-Fi 6. NR-U tested for various CAPs that were set with priority *p2* or *p4* at: (a) SCS 15 kHz, (b) SCS 30 kHz, and (c) SCS 60 kHz.

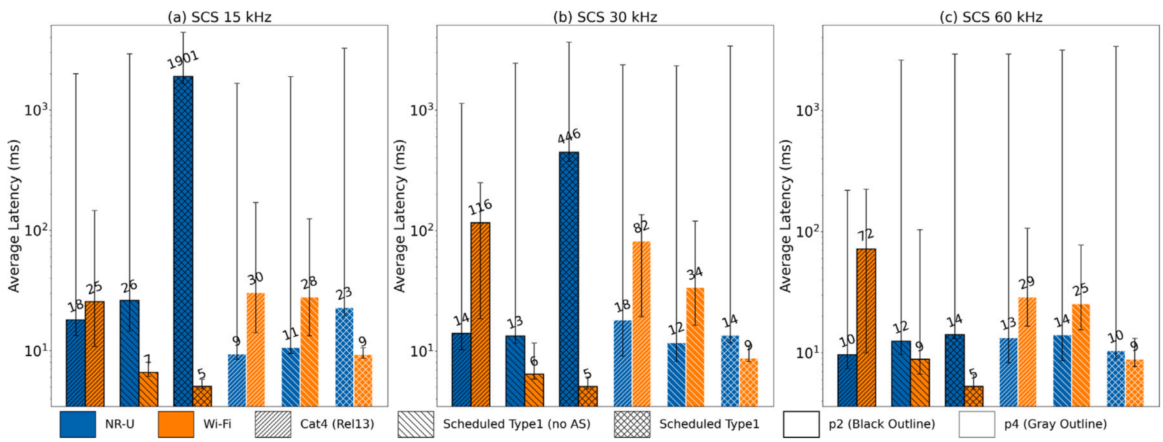

Fig. 9. Average latency performance for NR-U and Wi-Fi 6. NR-U was tested for various CAPs that were set with priority *p2* or *p4* at: (a) SCS 15 kHz, (b) SCS 30 kHz and (c) SCS 60 kHz in coexistence with Wi-Fi 6.

requirements can initially lead to higher BO but ultimately help reduce packet collision with Wi-Fi and, thus, the need for retransmissions. As SCS increases, Scheduled Type 1 CAP especially benefits from improved buffer servicing efficiency, leading to lower long-term BO levels.

Priority p4 at 60 kHz stands out for Scheduled Type 1, achieving a median BO below 55%, which aligns with a medium traffic load. At 15 kHz and 30 kHz, however, the same CAP and priority combination exceeds 55%, corresponding to high load conditions. For p2, the BO remains high at both 15 kHz and 30 kHz due to the short 3 ms MCOT not providing adequate time for servicing the RLC transmission buffers. Nonetheless, at 60 kHz, the BO for p2 is reduced by 28.8%, lowering saturation levels yet still falling into the high load category.

Overall, Scheduled Type 1 CAP gains the most from higher SCS values, as the lower probability of escalating to larger CWS outweighs the extra sensing overhead. Furthermore, while priority p4 consistently offers better performance than p2 in backoff and buffer occupancy, these results underscore the critical role of CAP priority selection in optimising NR-U coexistence with Wi-Fi networks.

5.3.3. Latency performance

Fig. 9(a), (b), and (c) display bar plots of the mean NR-U (blue bars) and Wi-Fi (orange bars) average end-to-end latency, with error bars indicating the 5th and 95th percentiles. These results are presented for NR-U operating under various CAPs set with priority p2 or p4 at an SCS of 15, 30, and 60 kHz, respectively.

The overall NR-U latency performance, depicted by the blue bars in Fig. 9(a), (b), and (c), shows that the lowest latency is achieved when implementing CAPs without AS, aligning with the observed BO levels in Fig. 8 for the same procedures. These results suggest that despite the higher packet collision rate attributed to the lack of AS, the less restrictive access to the channel compensates for this, allowing NR-U to achieve lower latencies. For the CAPs without AS and set with priority p4, latency performance degrades at larger SCSs due to longer backoff delays, as illustrated in Fig. 8. Conversely, lower latencies are achieved for the CAPs without AS and set with priority p2, which is less sensitive to the increased packet collisions at higher SCSs. Due to a better channel assessment of the scheduled LBT, the scheduled Type 1 CAP is the only procedure amongst the CAPs without AS for priority p2 that achieves a latency degradation similar to the CAPs set with priority p4.

Analysing the latency achieved by Scheduled Type 1 CAP reveals a similar performance enhancement as observed for the BO levels, demonstrating that at higher SCSs, increased channel access opportunities and improved interference prevention allow even the most conservative CAPs to achieve average latencies of under 15 ms. The CAP set with priority p2 achieves such latencies only at an SCS of 60 kHz, consistent with observed BO trends in Fig. 8.

Fig. 9(a), (b), and (c) show the median latency performance for the Wi-Fi network (orange bars), with error bars indicating the 5th and 95th percentiles, when NR-U implements various CAPs and priorities at an SCS of 15, 30, and 60 kHz, respectively. The Wi-Fi network achieves the lowest latency when using the EDCA set with AC_VI, and NR-U is set with the CAP with AS and priority p2 or priority p4 across all SCSs tested. The scheduled Type 1 CAP (no AS) set with priority p2 leads

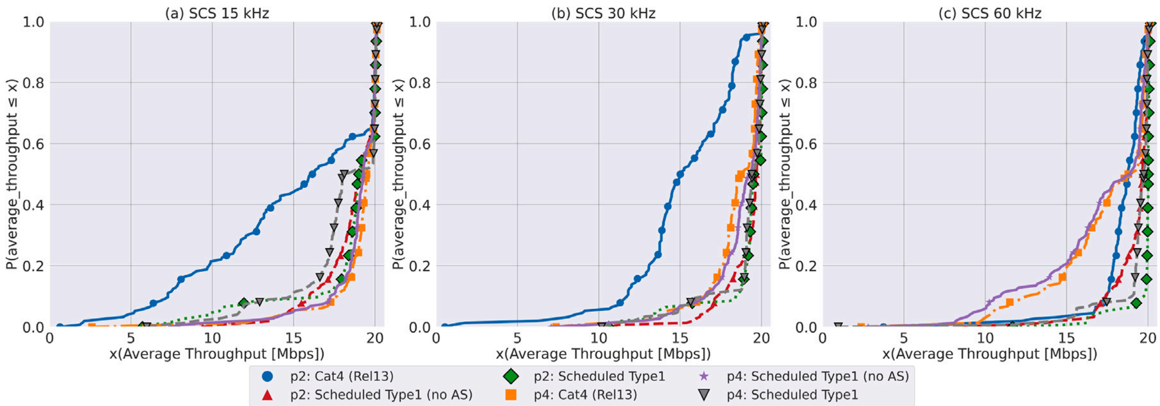

Fig. 10. Throughput performance of NR-U at various CAPs set with priority *p2* or *p4* at: (a) SCS 15 kHz, (b) SCS 30 kHz and (c) SCS 60 kHz in coexistence with Wi-Fi 6.

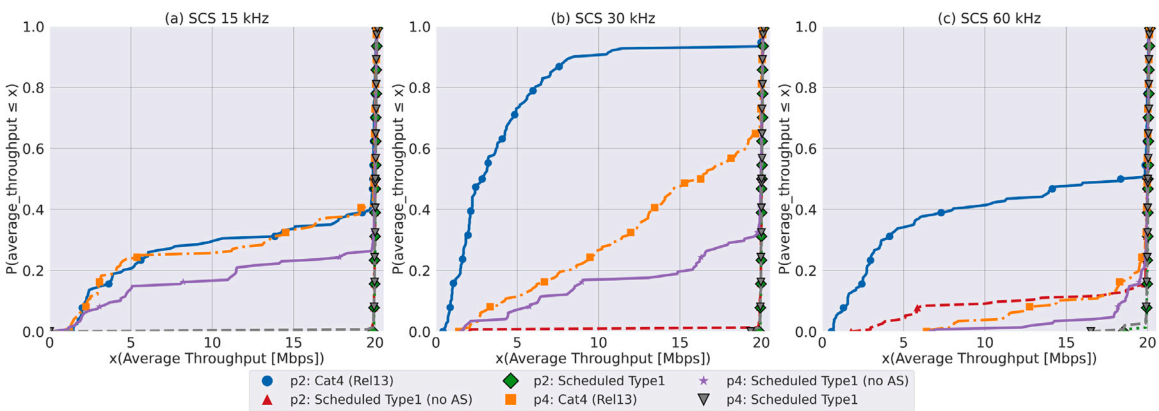

Fig. 11. Throughput Performance of Wi-Fi 6 when coexisting with NR-U at various CAPs set with priority *p2* or *p4* at: (a) SCS 15 kHz, (b) SCS 30 kHz and (c) SCS 60 kHz.

to Wi-Fi latencies below 10 ms. However, due to the lack of AS in this procedure, Wi-Fi latency performance degrades as NR-U SCS increases and more packets are lost, requiring the use of the channel more often. The lower latency observed for the Scheduled Type 1 CAP indicates that Wi-Fi performs best when NR-U has a lower MCOT, such as 3 ms for priority p2, compared to the 8 ms for priority p4. For p4, the NR-U scheduled Type 1 CAP is the only procedure at this priority level that leads to Wi-Fi latency of under 10 ms at an SCS of 15 and 30 kHz. A marginal degradation is observed for an SCS of 60 kHz, with tail results exceeding 20 ms. This shows that in cases where Type 1 CAP fails to prevent concurrent channel access, the larger MCOT of priority p4 in coexistence with AC_BE, which has an MCOT of 5.484 ms, leads to a higher latency degradation due to an uneven MCOT and share of the channel. Such occurrences are observed when the Wi-Fi network fails to detect NR-U transmission due to an ED threshold of −62 dBm, which is lower than the −72 dBm ED threshold at the NR-U network.

5.3.4. Throughput performance

This section analyses the average per-user throughput at the IP level for NR-U and Wi-Fi networks. Fig. 10(a), (b), and (c) present the average per-user throughput at the NR-U network using various CAPs set with priority p2 or p4 across SCS of 15, 30, and 60 kHz.

For Scheduled Type 1 CAP, a degradation in throughput is observed in the CDF region below the 50th percentile. This trend is consistent with the packet loss ratio observed for these CAPs. However, the throughput performance improves as the numerology increases, allowing the gNB to access the channel more frequently. This indicates that despite the increased level of sensing required by the scheduled Type 1 CAP, which can delay the gNB's access to the channel, these CAPs can achieve a throughput close to ideal at smaller slot durations.

For CAPs without AS, those set with priority p4 achieve the best performance at an SCS of 15 kHz due to low packet loss and sufficient channel access. However, at an SCS of 30 and 60 kHz, the throughput performance degrades due to higher packet collision rates that lead to larger CWS and higher backoff occupancy delays, lowering the channel access opportunities. Conversely, the CAPs without AS and set with priority p2 (excluding the scheduled CAP) perform the worst at an SCS of 15 and 30 kHz. This is attributed to their lower MCOT, which results in more frequent release and re-acquisition of the channel and increased TB loss due to the lack of AS. The shorter slot durations at an SCS of 60 kHz allow these procedures to transmit more packets, increasing the throughput. Amongst the CAPs without AS and set with priority p2, the scheduled Type 1 CAP (no AS) demonstrates the best performance across all SCSs, attributed to its lower packet loss.

Fig. 11(a), (b), and (c) depict the average throughput per user at the Wi-Fi network when NR-U uses various CAPs set with priority p2 or p4 tested for SCS of 15, 30, and 60 kHz.

The average throughput achieved in the Wi-Fi network with NR-U employing Scheduled Type 1 CAP demonstrates consistent and optimal performance across all tested SCS configurations. This underscores that differences in MCOT durations between NR-U priorities (p4 with MCOT 8 ms and p2 with MCOT 3 ms) and Wi-Fi's AC_BE (MCOT 5.484 ms) and AC_VI (MCOT 4 ms) do not decrease the average throughput. This robust performance is attributed to the Type 1 CAP implementation with the proposed scheduling technique that effectively prevents concurrent channel access in most scenarios.

In contrast, CAPs without AS lead to saturation of Wi-Fi throughput across all tested SCS settings, with the most pronounced impact observed at 30 kHz SCS. This saturation primarily results from Wi-Fi's payload duration of 0.608 ms, which aligns its transmission intervals with NR-U operating at 30 kHz SCS (slot duration of 0.5 ms). At

60 kHz SCS, CAPs without AS and set with priority p4 exhibit improved throughput in Wi-Fi due to their less frequent channel access. Amongst the CAPs without AS, Wi-Fi performs better when NR-U implements the scheduled Type 1 CAP (no AS) set with priority p2, leveraging an accurate assessment of the wireless channel by initiating backoff closer in time to the start of the transmission. This approach yields performance levels approaching those of Scheduled Type 1 CAP at 15 and 30 kHz SCS. However, at an SCS of 60 kHz, where NR-U experiences a higher number of TB lost, the lack of AS results in a noticeable degradation in the Wi-Fi's throughput performance.

6. Conclusion

In this work, we have proposed, implemented, and evaluated a standard-compliant NR-U SA model for the ns-3 network simulator, incorporating a novel Scheduled Type 1 CAP to access unlicensed channels shared with a coexisting Wi-Fi network. Our proposed Scheduled Type 1 CAP extends the 3GPP Type 1 CAP [11] by introducing a scheduling technique and implementing AS to seamlessly integrate the asynchronous Type 1 CAP into the NR-U synchronous system slot-based framework, addressing challenges of synchronisation gaps and misalignment with slot boundaries.

The Scheduled Type 1 CAP demonstrated its efficacy by maintaining low packet loss ratios, below 1% for Wi-Fi and 10% for NR-U SA. Its lower backoff occupancy and reduced BO level highlight its robustness against interference, thus, leveraging the benefits of higher SCS, such as increased channel access opportunities. While more restrictive than Cat4 LBT, the Scheduled Type 1 CAP provides fairer channel access. Although it initially increases latency, it effectively prevents packet loss, allowing the system to benefit from shorter slots and improved performance latency at higher SCS.

Performance evaluation revealed that, despite these improvements, NR-U SA cannot fully meet the QoS requirements for XR applications, particularly Cloud Gaming (CG). Latency exceeded 10 ms across all numerologies tested, with the best result, slightly surpassing the latency requirement, observed at 60 kHz SCS and priority *p4*. In contrast, Wi-Fi consistently met the 10 ms latency target, demonstrating superior performance. Further optimisation is needed for NR-U to fully meet latency-critical XR application requirements. This demonstrates that Wi-Fi, with its asynchronous transmission framework, outperforms the current NR-U framework.

Our analysis of non-compliant Cat4 LBT, predominantly used in the existing literature, showed that while it may reduce NR-U latency, it significantly degrades Wi-Fi performance, with packet loss ratios exceeding 50%. This highlights the importance of adhering to current 3GPP standards.

This study offers implementation insights that extend beyond 3GPP specifications, addressing gaps left for vendor-specific designs. By following these guidelines, researchers can ensure their work aligns with 3GPP standards, enhancing the validity of their work. These insights offer a strong foundation for further advancing NR-U and cellular-based access to unlicensed shared spectrum.

Future work will aim to explore methods such as NR-U mini-slot scheduling in deployments with a larger number of gNBs, where intra-RAT coexistence may exacerbate delays incurred during channel access. Increasing the granularity of channel access in NR-U could align its transmission behaviour more closely with that of Wi-Fi devices (i.e., load-based transmission) and achieve the performance necessary to support latency-critical XR application requirements.

Acknowledgements

CTTC authors have received funding from Grant PID2021-126431OB-I00 funded by MCIN/AEI/10.13039/501100011033 and “ERDF A way of making Europe”, and Generalitat Catalunya 2021 SGR 00770.

References

[1] R.K. Saha, Coexistence of cellular and IEEE 802.11 technologies in unlicensed spectrum bands -a survey, IEEE Open J. Commun. Soc. (OJ- COMS) 2 (2021) 1996–2028.

[2] 3GPP TSG RAN, Feasibility Study on 6 GHz for LTE and NR in Licensed and Unlicensed Operations, 3GPP TS 37.890 V19.0.0, 2024, URL https://www.3gpp.org/ftp/Specs/archive/37_series/37.890/.

[3] 3GPP TSG RAN, Study on Licensed-Assisted Access to Unlicensed Spectrum, 3GPP TR 36.889 V13.0.0, 2015, URL https://www.3gpp.org/ftp/Specs/archive/36_series/36.889/.

[4] S. Lagén, L. Giupponi, S. Goyal, N. Patriciello, B. Bojović, A. Demir, M. Beluri, New radio beam-based access to unlicensed spectrum: Design challenges and solutions, IEEE Commun. Surv. Tutor. 22 (1) (2020) 8–37.

[5] IEEE, Part 11: Wireless LAN Medium Access Control (MAC) and Physical Layer (PHY) specifications, IEEE Std 802.11, 2020, URL https://ieeexplore.ieee.org/document/9363693.

[6] ETSI, Harmonized EN Covering the Essential Requirements of Article 3.2 of the R&TTE Directive, ETSI EN 301 893 V1.8.1, 2015, URL https://www.etsi.org/deliver/etsi_en/301800_301899/301893/01.08.01_60/en_301893v010801p.pdf.

[7] ETSI, Harmonized Standard Covering the Essential Requirements of Article 3.2 of Directive 2014/53/EU, ETSI EN 301 893 V2.1.1, 2017, URL https://www.etsi.org/deliver/etsi_en/301800_301899/301893/02.01.01_60/en_301893v020101p.pdf.

[8] 3GPP TSG RAN, Evolved Universal Terrestrial Radio Access (E-UTRA); Physical Layer Procedures, 3GPP TS 36.213 V13.5.0, 2017, URL https://www.3gpp.org/ftp/Specs/archive/36_series/36.213/.

[9] S. Muhammad, H.H. Refai, M.O. Al Kalaa, 5G NR-U: Homogeneous coexistence analysis, in: Proc. Global Commun. Conf., Taipei, Taiwan, 2020, pp. 1–6.

[10] 3GPP TSG RAN, Study on NR-based Access to Unlicensed Spectrum, 3GPP TR 38.889 V16.0.0, 2018, URL https://www.3gpp.org/ftp/Specs/archive/38_series/38.889/.

[11] 3GPP TSG RAN, Physical Layer Procedures for Shared Spectrum Channel Access, 3GPP TS 37.213 V18.3.0, 2024, URL https://www.3gpp.org/ftp/Specs/archive/37_series/37.213/.

[12] GSMA, Harnessing spectrum diversity: GSMA policy position paper on licensed and unlicensed (or licence-exempt) spectrum, 2024, https://www.gsma.com/connectivity-for-good/spectrum/wp-content/uploads/2024/07/Licensed-and-unlicensed-spectrum-GSMA-Policy-Position-Paper.pdf.

[13] GSMA, Private 5G Industrial Networks: An Analysis of Use Cases and Deployment, GSMA White Paper, 2023, URL https://www.gsma.com/solutions-and-impact/technologies/internet-of-things/wp-content/uploads/2023/06/GSMA-Private-5G-Industrial-Networks-Report-June-2023.pdf.

[14] Qualcomm, Global 5G Spectrum Update and Innovations for Future Wireless Systems, Qualcomm White Paper, 2023, URL https://www.qualcomm.com/content/dam/qcomm-martech/dm-assets/documents/global-5g-spectrum-status-and-innovations-for-future-wireless-systems.pdf.

[15] AI-Linking, Industrial private 5G network, 2024, URL https://en.ailinking.com/IndustrialPrivate5GNetwork.

[16] A. Weissberger, 5G private networks, 2024, URL https://techblog.comsoc.org/category/5g-private-networks/.

[17] E. Pei, X. Lu, B. Deng, J. Pei, Z. Zhang, The impact of imperfect spectrum sensing on the performance of LTE licensed assisted access scheme, IEEE Trans. Commun. 68 (3) (2019) 1966–1978.

[18] E. Pei, L. Zhou, B. Deng, X. Lu, Y. Li, Z. Zhang, A Q-learning based energy threshold optimization algorithm in LAA networks, IEEE Trans. Veh. Technol. 70 (7) (2021) 7037–7049.

[19] E. Pei, Y. Huang, L. Zhang, Y. Li, J. Zhang, Intelligent access to unlicensed spectrum: a mean field based deep reinforcement learning approach, IEEE Trans. Wirel. Commun. 22 (4) (2022) 2325–2337.

[20] H. Zhou, Y. Deng, A. Nallanathan, Novel listen-before-talk access scheme with adaptive backoff procedure for uplink centric broadband communication, IEEE Internet Things J. 10 (22) (2023) 19981–19992.

[21] W. Wang, P. Xu, Y. Zhang, H. Chu, Performance analysis of LBT Cat4 based downlink LAA-WiFi coexistence in unlicensed spectrum, in: 2017 9th International Conference on Wireless Communications and Signal Processing, WCSP, IEEE, 2017, pp. 1–6.

[22] J. Xiao, J. Zheng, L. Chu, Q. Ren, Performance modeling and analysis of the LAA category-4 LBT procedure, IEEE Trans. Veh. Technol. 68 (10) (2019) 10045–10055.

[23] M. Parvini, A.H. Zarif, A. Nouruzi, N. Mokari, M.R. Javan, B. Abbasi, A. Ghasemi, H. Yanikomeroglu, Spectrum sharing schemes from 4G to 5G and beyond: Protocol flow, regulation, ecosystem, economic, IEEE Open J. Commun. Soc. 4 (2023) 464–517.

[24] M. Hirzallah, M. Krunz, B. Kecicioglu, B. Hamzeh, 5G new radio unlicensed: Challenges and evaluation, Trans. Cogn. Commun. Netw. 7 (3) (2020) 689–701.

[25] G.J. Sutton, R.P. Liu, Y.J. Guo, Harmonising coexistence of machine type communications with Wi-Fi data traffic under frame-based LBT, IEEE Trans. Commun. 65 (9) (2017) 4000–4011.

[26] A. Abdelfattah, N. Malouch, J. Ling, Analytical evaluation and potentials of frame based equipment for LTE-laa/wi-fi coexistence, in: 2019 IEEE Symposium on Computers and Communications (ISCC), IEEE, 2019, pp. 1–7.
[27] T.-K. Le, F. Kaltenberger, U. Salim, Dynamic switch between load based and frame based channel access mechanisms in unlicensed spectrum, in: 2021 IEEE Global Communications Conference, GLOBECOM, IEEE, 2021, pp. 1–6.
[28] N. Wei, X. Lin, Y. Xiong, Z. Chen, Z. Zhang, Joint listening, probing, and transmission strategies for the frame-based equipment in unlicensed spectrum, IEEE Trans. Veh. Technol. 67 (2) (2017) 1750–1764.
[29] G.J. Sutton, R.P. Liu, Y.J. Guo, Coexistence performance and limits of frame-based listen-before-talk, IEEE Trans. Mob. Comput. 19 (5) (2019) 1084–1095.
[30] V. Weerackody, H. Yin, S. Roy, NR sidelink mode 2 in unlicensed bands: Throughput model & validation, IEEE Trans. Commun. (2024).
[31] M. Hirzallah, M. Krunz, Y. Xiao, Harmonious cross-technology coexistence with heterogeneous traffic in unlicensed bands: Analysis and approximations, IEEE Trans. Cogn. Commun. Netw. 5 (3) (2019) 690–701.
[32] J. Peng, Y. Gao, X. Sun, W. Zhan, Z. Guo, 3GPP fairness constrained throughput optimization for 5G NR-U and wifi coexistence in the unlicensed spectrum, in: 2022 IEEE Wireless Communications and Networking Conference, WCNC, IEEE, 2022, pp. 1779–1784.
[33] M. Zając, S. Szott, Resolving 5G NR-U contention for gap-based channel access in shared sub-7 GHz bands, IEEE Access 10 (2022) 4031–4047.
[34] K. Kosek-Szott, A.L. Valvo, S. Szott, P. Gallo, I. Tinnirello, Downlink channel access performance of NR-U: Impact of numerology and mini-slots on coexistence with Wi-Fi in the 5 GHz band, Comput. Netw. 195 (2021) 108188.
[35] S. Szott, K. Kosek-Szott, A.L. Valvo, I. Tinnirello, Using self-deferral to achieve fairness between wi-fi and NR-U in downlink and uplink scenarios, Comput. Commun. 193 (2022) 176–188.
[36] A. Myles, Proposed LS to 3GPP RAN1 related to blocking energy, IEEE 802.11 Coexistence SC, 2019, URL https://mentor.ieee.org/802.11/dcn/19/11-19-1474-01-coex-ls-to-3gpp-ran1-about-blocking-energy.docx.
[37] L. Bertizzolo, E. Demirors, Z. Guan, T. Melodia, Cobeam: Beamforming-based spectrum sharing with zero cross-technology signaling for 5G wireless networks, in: IEEE INFOCOM 2020-IEEE Conference on Computer Communications, IEEE, 2020, pp. 1429–1438.
[38] C.B. Papadias, A.J. Paulraj, Space-time signal processing for wireless communications: a survey, in: First IEEE Signal Processing Workshop on Signal Processing Advances in Wireless Communications, IEEE, 1997, pp. 285–288.
[39] N. Patriciello, S. Lagen, B. Bojović, L. Giupponi, NR-U and IEEE 802.11 technologies coexistence in unlicensed mmWave spectrum: Models and evaluation, IEEE Access 8 (2020) 71254–71271.
[40] R. Maldonado, C. Rosa, K.I. Pedersen, Analysis of high-reliable and low-latency communication enablers for new radio unlicensed, in: 2020 IEEE Wireless Communications and Networking Conference, WCNC, IEEE, 2020, pp. 1–6.
[41] R. Maldonado, C. Rosa, K.I. Pedersen, A fully coordinated new radio-unlicensed system for ultra-reliable low-latency applications, in: 2020 IEEE Wireless Communications and Networking Conference, WCNC, IEEE, 2020, pp. 1–6.
[42] 3GPP TSG RAN WG1, Coexistence Evaluation Results for NR-Unlicensed, 3GPP TSG RAN WG1 Meeting #95, R1-1813409, Qualcomm Inc., 2018, URL https://www.3gpp.org/ftp/tsg_ran/wg1_rl1/TSGR1_95/Docs/.
[43] 3GPP TSG RAN WG1, Channel Access Mechanisms for NR-U, 3GPP TSG RAN WG1 Meeting #95, R1-1814020, Ericsson, 2018, URL https://www.3gpp.org/ftp/tsg_ran/wg1_rl1/TSGR1_95/Docs/.
[44] 3GPP TSG RAN WG1, Evaluation Results for NR-U, 3GPP TSG RAN WG1 Meeting #95, R1-1814074, Samsung, 2018, URL https://www.3gpp.org/ftp/tsg_ran/wg1_rl1/TSGR1_95/Docs/.
[45] 3GPP TSG RAN WG1, Evaluation Results for NR-U, 3GPP TSG RAN WG1 Meeting #95, R1-1812659, Nokia, 2018, URL https://www.3gpp.org/ftp/tsg_ran/wg1_rl1/TSGR1_95/Docs/.
[46] N. Patriciello, S. Lagen, B. Bojovic, L. Giupponi, An E2E simulator for 5G NR networks, Simul. Model. Pr. Theor. J. 96 (2019) 101933.
[47] K. Koutlia, B. Bojovic, Z. Ali, S. Lagén, Calibration of the 5G-LENA system level simulator in 3GPP reference scenarios, Simul. Model. Pr. Theor. J. (ISSN: 1569-190X) 119 (2022) 102580, http://dx.doi.org/10.1016/j.simpat.2022.102580.
[48] 3GPP TSG RAN, Study on New Radio (NR) Access Technology, 3GPP TR 38.912 V18.0.0, 2024, URL https://www.3gpp.org/ftp/Specs/archive/38_series/38.912/.
[49] 3GPP TSG RAN, Study on XR (Extended Reality) Evaluations for NR, 3GPP TR 38.838 V17.0.0, 2021, URL https://www.3gpp.org/ftp/Specs/archive/38_series/38.838/.
[50] S. Lagen, B. Bojovic, K. Koutlia, X. Zhang, P. Wang, Q. Qu, QoS management for XR traffic in 5G NR: A multi-layer system view & end-to-end evaluation, IEEE Commun. Mag. (2023).
[51] TSG RAN WG1, Considerations on Performance Evaluation for NR in 52.6-71GHz, Intel Corporation, 2020, URL https://www.3gpp.org/ftp/tsg_ran/WG1_RL1/TSGR1_103-e/Docs.

George V. Frangulea received the MEng (Hons) degree in electronic and communications engineering from the University of Kent, Canterbury, UK, in 2020, where he is currently pursuing a PhD in electronic engineering. In 2023, he secured UKRI funding for research in industrial IoT solutions over unlicensed spectrum. He has contributed to multiple open-source initiatives on NR-U simulation models for ns-3. His research interests include radio frequency coexistence, MIMO transmission technologies, and multi-rat spectrum sharing (MRSS) for 5G and beyond.

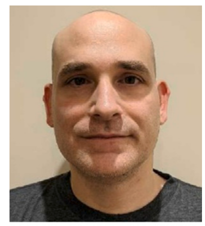

Philippos Assimakopoulos received the B.Eng. degree in electronic engineering from the University of Bath, Bath, UK, in 2003, and the M.Sc. degree in broadband and mobile communication networks and Ph.D. degree in electronic engineering from the University of Kent, Canterbury, UK, in 2007 and 2012, respectively. He is currently a lecturer with the Communications Research Group, University of Kent. He has participated as Co-I and PI in several EU FP7, Horizon 2020, UK EPSRC and industrial collaboration research projects and was a voting member of the IEEE1914 working group ("Next Generation Fronthaul Interface") for a number of years. He has co-authored two book chapters, including in the seminal book on 5G ("5G system design, Wiley publishing house"), has a granted patent (on methods for generating and processing a transport signal in a radio access network) and was the co-recipient of the Fabio Neri Best Paper Award for best research paper published in 2021 (Elsevier OSN journal). His research interests include distributed antenna systems and low-cost microwave radio-over-fiber networks for indoor and outdoor applications and the design of radio access network for 5G and beyond.

Biljana Bojović received her M.Sc. in Electrical and Computer Engineering from the Faculty of Technical Sciences, Novi Sad, Serbia, in 2008 and her Ph.D. in Networking Engineering from the Polytechnic University of Catalonia, Barcelona, Spain, in 2022. In 2009, she joined CTTC research center, in Spain, where she is currently a Senior Researcher and Scientific Promoter of the OpenSim research unit. She is the developer and maintainer of the NR, NR-U, and LTE modules of the ns-3 network simulator and the principal author of the LAA and LTE-U modules. She held LTE and NR module tutorials at the ns-3 workshops in 2016, 2022, and 2024 and at CONFTELE in 2021. In addition, she was a mentor of ns-3 GSoC on several occasions. In 2020 she received the ACM SIGCOMM Networking System Award. She worked on many research projects for industrial clients, such as Wi-Fi Alliance, SpiderCloud, Interdigital, the US Department of Defense, NIST, Meta (Facebook), etc. She is a co-author of one patent application (US20200314906A1). Her research interests include XR traffic enhancements for 5G-Advanced, MIMO simulation models for ns-3, and unlicensed/shared spectrum.

Sandra Lagén received her B.Sc., M.Sc. and Ph.D. degrees from Universitat Politècnica de Catalunya (UPC), Spain, in 2011, 2013, and 2016, respectively. Her dissertation was awarded by COIT the best national Ph.D. thesis on high-speed broadband mobile communications (2017) and received a Special Doctoral Award by UPC (2019). In 2017, she joined CTTC research center, Spain, where she is currently a Senior Researcher and Head of the Open Simulations (OpenSim) research unit. She has led and participated in outstanding direct collaborative projects with major telecom industry players (including InterDigital, Huawei, Meta, and others), US governmental agencies, as well as national and European funded projects. Also, she coordinates the design and developing team of ns-3 5G-LENA simulator. She is recipient of IEEE WCNC 2018 and WNS3 2020 best paper awards, and co-author of 2 non-provisional and 3 provisional patent applications. From 2021 to 2024, she was a member of the executive board of the ns-3 consortium. Her research interests include wireless communications, spectrum and interference management, optimization theory, and cross-layer system design.